RESEARCH ARTICLE

2-Methyl-4-chlorophenoxyacetic acid (MCPA) sorption and desorption as a function of biochar properties and pyrolysis temperature

Abdullah Niaz [1,2], **Kurt A. Spokas** [3]*, **Bea Gámiz** [4], **David Mulla** [2], **Khaliq R. Arshad** [1], **Sarfraz Hussain** [1]

1 Pesticide Residue Laboratory, Institute of Soil Chemistry & Environmental Sciences, Kala Shah Kaku, Punjab, Pakistan, **2** Department of Soil, Water and Climate, University of Minnesota, St. Paul, MN, United States of America, **3** United States Department of Agriculture, Agricultural Research Service, St. Paul, MN, United States of America, **4** Department of Inorganic Chemistry, Chemical Institute for Energy and the Environment (IQUEMA), University of Córdoba, Córdoba, Spain

* kurt.spokas@usda.gov

Abstract

2-Methyl-4-chlorophenoxyacetic acid (MCPA) is a highly mobile herbicide that is frequently detected in global potable water sources. One potential mitigation strategy is the sorption on biochar to limit harm to unidentified targets. However, irreversible sorption could restrict bioefficacy thereby compromising its usefulness as a vital crop herbicide. This research evaluated the effect of pyrolysis temperatures (350, 500 and 800°C) on three feedstocks; poultry manure, rice hulls and wood pellets, particularly to examine effects on the magnitude and reversibility of MCPA sorption. Sorption increased with pyrolysis temperature from 350 to 800°C. Sorption and desorption coefficients were strongly corelated with each other ($R^2 = 0.99$; $P < .05$). Poultry manure and rice hulls pyrolyzed at 800°C exhibited irreversible sorption while for wood pellets at 800°C desorption was concentration dependent. At higher concentrations some desorption was observed (36% at 50 ppm) but was reduced at lower concentrations (1–3% at < 5 ppm). Desorption decreased with increasing pyrolysis temperature. Sorption data were analyzed with Langmuir, Freundlich, Dubinin–Radushkevich and Temkin isotherm models. Freundlich isotherms were better predictors of MCPA sorption (R^2 ranging from 0.78 to 0.99). Poultry manure and rice hulls when pyrolyzed at higher temperatures (500 and 800°C) could be used for remediation efforts (such as spills or water filtration), due to the lack of desorption observed. On the other hand, un-pyrolyzed feedstocks or biochars created at 350°C could perform superior for direct field applications to limit indirect losses including runoff and leaching, since these materials also possess the ability to release MCPA subsequently to potentially allow herbicidal action.

Introduction

Extensive pesticide use has severely affected the quality of soil, water and air, bringing undesirable impacts, including toxicity and carcinogenicity, on non-target species including humans

[1]. Pesticide contamination could negatively affect soil quality, nutrient cycling, enzyme activity, soil biota, biodiversity and endangering other ecosystem processes [2]. There is always a potential risk of groundwater pollution and pesticides being the most intensively observed chemicals in European groundwater [3]. Recent research has shown pesticide residues in 60% of studied groundwater samples, from both urban and agricultural farms in the United States [4]. 2-Methyl-4-chlorophenoxyacetic acid (MCPA) is a hormone-type, selective, systemic herbicide, readily absorbed by roots and leaves, to be used for controlling annual as well as perennial weeds in grassland, cereals and turf [5]. Additionally, MCPA is used to control aquatic broad leaf weeds [6]. MCPA is a weak organic carboxylic acid with a pK_a value of 3.1, meaning that it will predominantly be in its anionic form at typical soil pH values (between 5 to 8) [7]. More than 2,000 t of MCPA are used only in Western Europe each year [8]. MCPA is highly mobile in soils, with K_{oc} from 50 to 62 L kg^{-1} and has a short to moderate 7 to 41 day half-life [9,10]. These two factors suggest that MCPA has a potential risk for contaminating potable water sources [11,12]. In fact, MCPA is one of the most widespread pesticides detected globally in lakes, rivers, and groundwater [13–15].

Biochar, a carbon-enriched product, comes from the thermal decomposition of organic material, including animal manure [16], crop residues [17], woody materials [18], biosolids [19], industrial by-products, urban-yard wastes and sewage sludge [20]. These carbon-rich materials due to biomass pyrolysis have been reported to increase crop yields through enhanced water-holding capacity and nutrient availability [21,22] and are a means of sequestering carbon in soil [23]. Sorption of organic and inorganic pollutants by biochar is due to aromaticity and higher surface area [24], large pore structure, diverse surface functional groups, high pH, and high cation exchange capacity [25]. Several studies have established sorption of various pesticides on biochar [18,26] and showing biochar can be a "super-sorbent" for contaminants [27]. Sorption on biochar could have numerous benefits, including, reducing leaching and runoff losses [28]. However, at the same time biochar can retain pesticides in soils for longer periods due to retarding pesticide dissipation [29,30] and protecting pesticides from microbial mineralization [28,31].

Another important environmental issue worldwide could be agricultural wastes being produced globally in millions of tons every year [32]. The worldwide burning of annually generated crop residues could cause very large environmental risk, producing atmospheric pollution and significant carbon particulates. In India alone, the total estimated annual crop residues left-over is about 141 Mt, out of this 93 Mt crop residues were burnt on-farm [33]. Crop residues could be low-cost feedstocks for biochar and an alternative for managing agricultural waste. This approach is quite sustainable and economically feasible for converting wastes into biochar [34]. Studies have shown that biochars from wood, wheat and rice residues could be 400–2500 times more effective than the original soil for pesticide sorption [35].

Sorption capacity of biochar might not be as high as other types of sorbents, like activated carbon or even clays (i.e., smectite) [36,37]. So, modifications of biochar, to enhance its sorption capacity, have also been reported, including loading organic functional groups and alkali activation [38,39], mineral loading on biochar such as magnetite, hematite, manganese oxide, zero valent Fe, and calcium oxide [28]. Additionally, studies have incorporated nanoparticles, such as nanocrystals of ZnS [40] or loading 1% graphene on the biochar surface [41]. However, if these modified biochars are applied to soil, it is important to consider not only economic viability, but also the need to evaluate potential contamination by the various activating agents [28]. Contrary to other comparatively complex ways for increased pesticide sorption, merely selecting an appropriate feedstock and variation in pyrolysis temperature during biochar preparation could optimize pesticide sorption on biochar surfaces [42–45]. It has been established that biochar application effects in soils depend mainly on the feedstock and pyrolysis temperature [46,47].

Longer persistence and reduced mobility of pesticides due to sorption on biochar could reduce the efficacy of soil-applied pesticides, especially that of herbicides [48], making weed control more problematic [49]. Therefore, there are two aspects of pesticide sorption on biochar. On one side, it might be considered favorable, thereby reducing the leaching, bioavailability and the non-target toxicity due to pesticides in soil [50]. While on the other, reduced bioavailability can be problematic in an agricultural setting, since it can reduce the plant uptake and efficacy of pre-emergent herbicides, requiring the farmer to apply more pesticides/herbicides on a biochar-amended field [51].

Therefore, better knowledge about locally available feedstocks and how various pyrolysis temperatures affect adsorption-desorption properties are needed to guide selection of biochar properties to improve adsorption to protect the environment, while allowing some desorption back to the soil solution, thereby maintaining good bioefficacy for weed control. The present study aimed to characterize and compare biochars, for MCPA sorption and desorption abilities. Three biomass residues were studied; poultry manure, rice hulls and wood pellets, subjected to three pyrolysis temperatures (350, 500 and 800˚C). The hypothesis is that MCPA sorption and desorption potentials can be optimized by specific combinations of feedstock and pyrolysis temperature.

Materials and methods

Chemicals

Radiolabeled ^{14}C material of 4-chloro-2 methylphenoxy acetic acid sodium salt monohydrate (MCPA; CAS [3653-48-3]) was obtained from Moravek, Inc. (MC-2515; Brea, CA USA). Radiolabeled MCPA [ring-U-^{14}C] had a specific activity of 12.3 MBq mg^{-1}. Additionally, non-labelled MCPA was obtained from ChemService, Inc. (N-10818-250MG; PA, USA) and reagent grade (99% purity) of $CaCl_2$ dihydrate was obtained from Sigma-Aldrich (223506; St. Louis, MO USA). A summary of the key properties of MCPA is given in Table 1.

Biochars

Three different feedstocks [poultry manure (PM), rice husks (RH) and wood pallets (WP)] were used to prepare the biochars for evaluation. These were coded with the two-letter feedstock followed by pyrolysis temperature in˚C or RAW in subscript designating the original non-pyrolyzed feedstock. A total of 12 different sorbents, including raw form and biochars created at three pyrolysis temperatures (350, 500 and 800˚C) were named as; PM$_{RAW}$, PM350, PM500, PM800, RH$_{RAW}$ RH350, RH500, RH800, WP$_{RAW,}$ WP350, WP500 and WP800. Prior to pyrolysis, the feedstocks were oven dried for 24 h at 60˚C, followed by mechanical sieving to < 4 cm. The feedstocks were pyrolyzed using a box furnace-retort system (Lindberg/MPH, Riverside, MI), between 0.5 and 1.5 kg of ground material was loaded onto a stainless-steel tray or into a crucible and placed into a gas tight retort for 2 h under a stream of N_2 gas at the

Table 1. Key properties of MCPA.

Characteristics	Value
Density 20 ˚C (g cm^{-3})	1.56
Solubility 20 ˚C (mg L^{-1})	270,000
Negative logarithm of the acid dissociation constant (pK$_a$ = -log K$_a$)	3.1 [7]
Soil half-live (t$_{1/2}$; days)	7–41 [9,10]
Soil sorption coefficient (K$_D$; L kg^{-1})	0.3–1.5 [52–55]

https://doi.org/10.1371/journal.pone.0291398.t001

desired pyrolytic temperature. The samples were stored in sealed low density polyethylene film (LDPE) bags (Ziploc[TM]) until use (< 6 months from the time of biochar production).

Characterization of biochars

Loss on drying was determined in air at 105˚C overnight and is reported on an as received sample basis. All other results are reported on a dried sample basis. Elemental (C, H, N, and O) analysis was carried out using thermal combustion (Hazen Research, Golden, CO USA). Ash percentage was determined after heating to 750˚C in air and holding at temperature for 8 h. Molar ratios of C:N, H:C, and O:C were also calculated from the elemental composition data. The Fourier-transform infrared (FTIR) spectroscopy data were collected using the attenuated total reflection (ATR; ThermoFisher iS50 FTIR spectrometer). The ATR used a diamond crystal. In the data collection, the resolution was 2 cm^{-1} and the number of scans for each spectrum was 32. The averaged spectrum from each sample was then displayed on an absorbance scale. Surface analyses were performed by nitrogen sorption analysis (MSE Analytical Services, Tucson, AZ, USA). Samples were degassed at 250˚C for 8 h prior to analysis. Surface areas were estimated at -196˚C using N_2 and the Brunauer–Emmett–Teller method, based on the best linear fit for points in the 0.025–0.30 P/P$_0$ range [56]. Total pore volume was estimated through the Barrett-Joyner-Halenda (BJH) method on the N_2 absorption data [57]. Scanning electron micrographs were also collected for the biochars and feedstocks. The physico-chemical properties of studied biochars were also correlated with MCPA sorption and desorption K_D to assess for any significant relationships.

Sorption study

Sorption was measured by laboratory batch sorption experiments, according to modified OECD 106-Tier 3 guidelines (OECD, 2000). Each sorbent (0.25 g dry weight) was mixed with different volume combinations of 0.01 M $CaCl_2$ and unlabeled MCPA (S1 Table in S1 Text) followed by a fixed volume of ^{14}C-labelled MCPA, to achieve multiple initial concentrations of 0.1, 0.9, 4.7, 9.4, 25 and 50 µg MCPA mL^{-1}, which corresponds to 450,000 Bq per vial (8,440 DPM mL^{-1}) over the range of MCPA concentrations. These sorption experiments were conducted in triplicate.

Each sorbent was placed in 20-mL glass scintillation vials, followed by the corresponding liquid injections from S1 Table in S1 Text, which were then placed horizontally on a reciprocal shaker and allowed to equilibrate for 24 h (180 rev min^{-1}) in the dark. Following this period, the samples were centrifuged (20 min, 1,500 × g), a sample of supernatant (1 mL) was removed and filtered through 0.45 µm syringe filter. Then a 0.20-mL aliquot of the filtered solution was mixed with 6 mL of scintillation cocktail [EcoLite(+); MP Biomedicals, LLC] and analyzed for ^{14}C by liquid scintillation counting (LSC) (HITACHI AccuFLEX LSC-8000, GMI Ramsey, MN; 10-min counting window). No statistically significant sorption of MCPA to scintillation vials, syringes, pipette tips, or syringe filters was observed (88–100% recovery; data not shown). Additionally, previous studies with MCPA have not detected significant degradation in laboratory incubations in 24 h [58]. The MCPA sorbed concentration on biochar (C_s; µg g^{-1}) was estimated by the following:

$$C_S = \frac{(C_i - C_e)V}{m},$$

where C_i is the initial MCPA concentration (µg mL^{-1}), C_e is the equilibrium MCPA concentration (µg mL^{-1}), V is the total volume of the liquid phase (mL), and m is the mass of the biochar (g). The liquid concentration was determined by the LSC of the liquid phase using the following

equation:

$$C_e = \frac{(LSC_e - Blank)C_i}{LSC_i},$$

where LSC_e is the disintegrations per minute of the sample following equilibration with the biochar, Blank is the disintegrations per minute (DPM) of the scintillation cocktail and vial alone, C_i is the liquid phase concentration of the initial standard (μg mL^{-1}), and LSC_i is the blank corrected DPM of the corresponding MCPA standards (without biochar; 8,440 DPM mL^{-1}).

Average liquid (C_e) and solid (C_s) concentrations were calculated from the three replicates and then analyzed by fitting to four different sorption models: Langmuir, Freundlich, Temkin, and the Dubinin–Radushkevich models by the R package *PUPAIM* [59]. The individual isotherm models are given in (S2 Table in S1 Text). All isotherm models were fitted using nonlinear regression curve fitting in R using the PUPAIM package [59]. An example R script for performing the isotherm fitting is provided in the Supplemental Information, including the graphical output (see S2 Text). The Langmuir isotherm is based on monolayer sorption to a fixed number of homogeneous sorption sites, with the maximum sorption capacity estimated by the coefficient Q_m. The value of the Freundlich coefficient $\frac{1}{n}$ provides insight into the distribution of sorption site heterogeneity with values closer to zero indicating higher degree of site heterogeneity. Although not theoretically derived, $\frac{1}{n}$ values of close to zero have been attributed to chemisorption and greater than one to more cooperative sorption mechanisms [60,61], meaning that the presence of adsorbates on the absorbent's surface enhances the adsorption processes. Additionally, the $\frac{1}{n}$ values have been correlated with the physio-chemical properties of the adsorbent [62]. The Temkin model expects indirect adsorbate/adsorbate interactions on the adsorption process, and provides an estimated heat of adsorption through the value of its coefficient B_t [63]. The Dubinin–Radushkevich isotherm is an empirical relationship focused on a pore filling mechanism and has been applied to sorption by microporous materials [64]. An estimated mean free energy of sorption (E; J mol^{-1}) can be estimated from the coefficient K_{DR} with the following relationship [64]:

$$E = \frac{1}{\sqrt{2K_{DR}}}.$$

Desorption study

A 5-mL aliquot of supernatant was removed after the first 24-h equilibration period and the initial adsorption was determined. Desorption of MCPA was accomplished by replacing the 5-mL aliquot removed from the equilibrated vial with 5 mL of fresh 0.01 M CaCl$_2$, at each concentration tested for sorption. The vials were vortexed to disperse the biochar sample back into the solution, mechanically shaken as previously described for 24 h, and then recentrifuged. The concentration of MCPA present in the aqueous solution after the 24-h desorption period was determined by LSC, as previously described, except for using 0.5 mL of the filtered supernatant for LSC counting. The desorption isotherm was fitted to the Freundlich model and compared to the original sorption isotherms. Specifically, the hysteresis (H) for MCPA sorption was quantified using formula using the Freundlich isotherm coefficients [65]:

$$H = \frac{\left(\frac{1}{n}\right)_{desorption}}{\left(\frac{1}{n}\right)_{sorption}}.$$

The H coefficient has values between 0 for a completely irreversible processes and 1 when the sorption isotherm follows the same pathway as sorption (reversible).

Statistical analysis

All data for the K_D determination were conducted in triplicate, with means and standard deviations of the measurements presented. All statistical analyses were performed in R [66]. The data for the isotherm analysis were analyzed for each biochar using the R package *PUPAIM* [59], which calculates the corresponding model isotherm coefficients as well as the root mean square error (RMSE), mean absolute error (MAE), Akaike Information Criterion (AIC), Bayesian Information Criterion (BIC), and the corresponding Pearson's correlation (R^2) of the model fits. The model with the lowest overall AIC, BIC, MAE, and RMSE over all the samples was correspondingly selected as the best-fitting isotherm model for the data. Correlation analysis was performed utilizing the R package *ggcorrplot* [67] to evaluate relationships between the soil chemical and physical properties and the resulting sorption coefficients. Two-way ANOVA and Tukey's HSD (Honestly Significant Difference) tests were used to compare K_D as a function of feedstock type and pyrolysis temperatures with the *agricolae* package [68] in R.

Results and discussion

Examination of biochar properties

The physical, chemical, and elemental properties of the biochars and original feedstocks are presented in Table 2. The observed air-dried moisture content of the raw feedstock samples showed poultry manure being the highest (7.3%) followed by rice hulls (5.5%) and wood pellets (4.3%). Higher pyrolysis temperatures reduced the air-dried moisture content, which was ascribed to the pyrolysis process itself altering the pore-structure of the various feedstocks. The volatilization of organic matter, water loss during dehydration, and collapse as well as fracturing during pyrolysis give birth to differing pore distributions in biochar as compared to the

Table 2. Elemental analysis and physico-chemical properties of feedstocks and biochars.

Biochar	Drying Loss	C	H	N	S	Ash	O	Volatile Matter	Fixed C	Molar Ratios					
										C:N	H:C	O:C	SSA	Pore Volume	pH
						% (w/w)								$(m^2 \, g^{-1})$	$(cm^3 \, g^{-1})$	
PM$_{Raw}$	7.32	36.48	4.92	2.93	1.33	24	37.1	61.75	14.26	14.5	1.62	0.76	0.1	0.001	6.1
PM350	2.04	39.58	2.76	3.27	1.63	47.6	19.9	28.54	23.82	14.1	0.84	0.38	3.3	0.001	6.2
PM500	1.92	35.84	1.28	2.45	2.17	61.9	14.7	17.73	20.41	17.1	0.43	0.31	5.1	0.002	7.4
PM800	4.15	41.55	0.71	1.8	1.96	66.4	12.2	9.13	24.5	26.9	0.21	0.22	61.6	0.025	9.4
RH$_{Raw}$	5.48	41.4	5.13	0.4	0.04	17.1	39.8	65.9	17.05	120.8	1.49	0.72	0.4	0.001	7.6
RH350	2.39	49.9	3.04	0.63	0.03	32	20.5	27.69	40.32	92.4	0.73	0.31	5.3	0.002	7.2
RH500	1.93	51.7	1.93	0.6	0.02	39.3	19.5	12.32	48.39	100.5	0.45	0.28	18.0	0.007	7.1
RH800	1.9	53.35	0.66	0.56	0.25	43.8	13.9	4.69	51.55	111.1	0.15	0.20	2.3	0.004	7.9
WP$_{Raw}$	4.26	50.36	6.14	0.07	0.01	0.37	46.3	82.42	17.21	839.3	1.46	0.69	0.1	0.003	5.5
WP350	2.46	76.39	3.8	0.18	0.01	1.01	20.4	32.9	66.09	495.1	0.60	0.20	0.6	0.003	5.4
WP500	1.76	89.12	2.82	0.18	0.01	1.34	8.72	15.15	83.51	577.6	0.38	0.07	0.2	0.004	5.8
WP800	0.91	95.66	0.85	0.37	0.1	1.67	2.51	4.2	94.12	301.6	0.11	0.02	46.6	0.018	6.5

Notes: PM = Poultry manure; RH = Rice hulls; WP = Wood pellets; Subscripted RAW = Raw and unpyrolysed feedstocks; Numerical suffixes = Pyrolysis temperatures at 350˚C, 500˚C and 800˚C. pH was determined by placing 0.25 g of each material in 3.2 mL of 0.01 M CaCl$_2$ then equilibrated for 24 hr. SSA is the specific surface area.

original feedstock [69]. As seen in Table 2, increasing pyrolysis temperature enhanced surface area as well as the estimated total pore volume. Although these increases were the greatest in the PM and WP feedstocks (Table 2). Pyrolysis processes are often complicated by the presence of various inorganic species [70], which could be an important facet determining the pyrolysis reactions for poultry manure and rice hulls.

Samples of biochars from PM and RH possessed higher ash content, due to higher amounts of inorganic species in the ash, which would result in oxygen being included in both the direct oxygen analysis and ash analysis results. The elemental analysis (C, H, N, S, and O) determined that WP contained higher C (total and fixed) than other samples (P<0.05). Carbon content typically increased with pyrolysis temperatures, although not statistically significant across all temperatures and feedstocks (P>0.05). The increased carbon contents at higher temperatures have been documented in prior studies [e.g., 44]. Heitkötter and Marschner [71] observed higher carbon contents at 600°C pyrolysis temperature than 400°C and importantly, the effect of heating was more pronounced in case of woody, pine chip-based biochars than in corn-based biochars. This was also observed in our study, where carbon contents increased more dramatically for wood pellet biochars compared to other two feedstocks: PM and RH. There was a strong correlation between C content and fixed carbon (R = 0.955; P<0.01).

Poultry manure showed higher N (2.9%) among the feedstocks which decreased with increases in pyrolysis temperature, suggesting a loss of volatile N compounds with the increasing pyrolysis temperatures. On the other hand, for two other materials, rice hulls and wood pellets, N contents increased slightly with increasing temperature, suggesting the N was conserved during the pyrolysis process with the loss of more volatile constituents. Overall, there was a correlation between N and S contents (R = 0.885; P<0.01).

Among these feedstocks, poultry manure gave higher ash contents (24%) and ash contents increased with higher pyrolysis temperatures which could result in higher pH (Table 2) [72]. A more alkaline biochar could be a result of carbonate species and/or and base cations [73], while corresponding reducing acidic functional groups like -COOH on biochar [74] (Fig 1). Such decreases in carboxylic acid groups, correlated to the increase in ash contents, has already been reported for both; manure-based biochars on pyrolysis temperature increasing from 300 to 500°C [42] as well as plant residues-based biochars, including soybean, corn, canola and peanut straw when subjected to pyrolysis at 700°C, compared to biochars at 300°C [73].

The C:N ratio was higher for both plant sources than poultry manure, highest (839) with wood pellets and increase in pyrolysis temperature decreased N contents with poultry manure, showing little variation until rapidly increasing at the highest pyrolysis temperature. The H:C ratio decreased with increasing temperature, which corresponds to increasing carbon-carbon bonding and decreasing surface moieties [75]. According to Cely et al. [76], biochar that is produced at temperatures above 400°C typically have a H:C ratio that is less than 0.5 and will further decrease with increasing pyrolysis temperatures. This was observed here with pyrolysis temperatures above 500°C having a H:C ratio less than 0.5 for all three feedstocks (Table 3). There was a strong relationship between H:C and O:C ratios (R = 0.952, P<0.01). These ratios suggest that the resulting carbon structures are being dominated by carbon-carbon bonds without extensive surface functional groups as pyrolysis temperature increases. This was also confirmed in the FTIR data, where it is clearly seen that the carbon-oxygen and carbon-hydrogen bonds become less abundant as the pyrolysis temperature is increased across all the feedstocks (Fig 1). As seen in the FTIR spectra for the 800°C pyrolysis biochars, there are no peaks corresponding to the aromatic carbon double bonds (1,580 cm^{-1}) or a band due to the stretching vibrations of aromatic carbon (3,045 cm^{-1}) [77,78]. These observations coupled with the low H:C ratio suggests there is no hydrogen atoms that are bonded to the carbon atoms within the biochar, thereby suggesting a structure with predominantly covalent C-C bonds (e.g.,
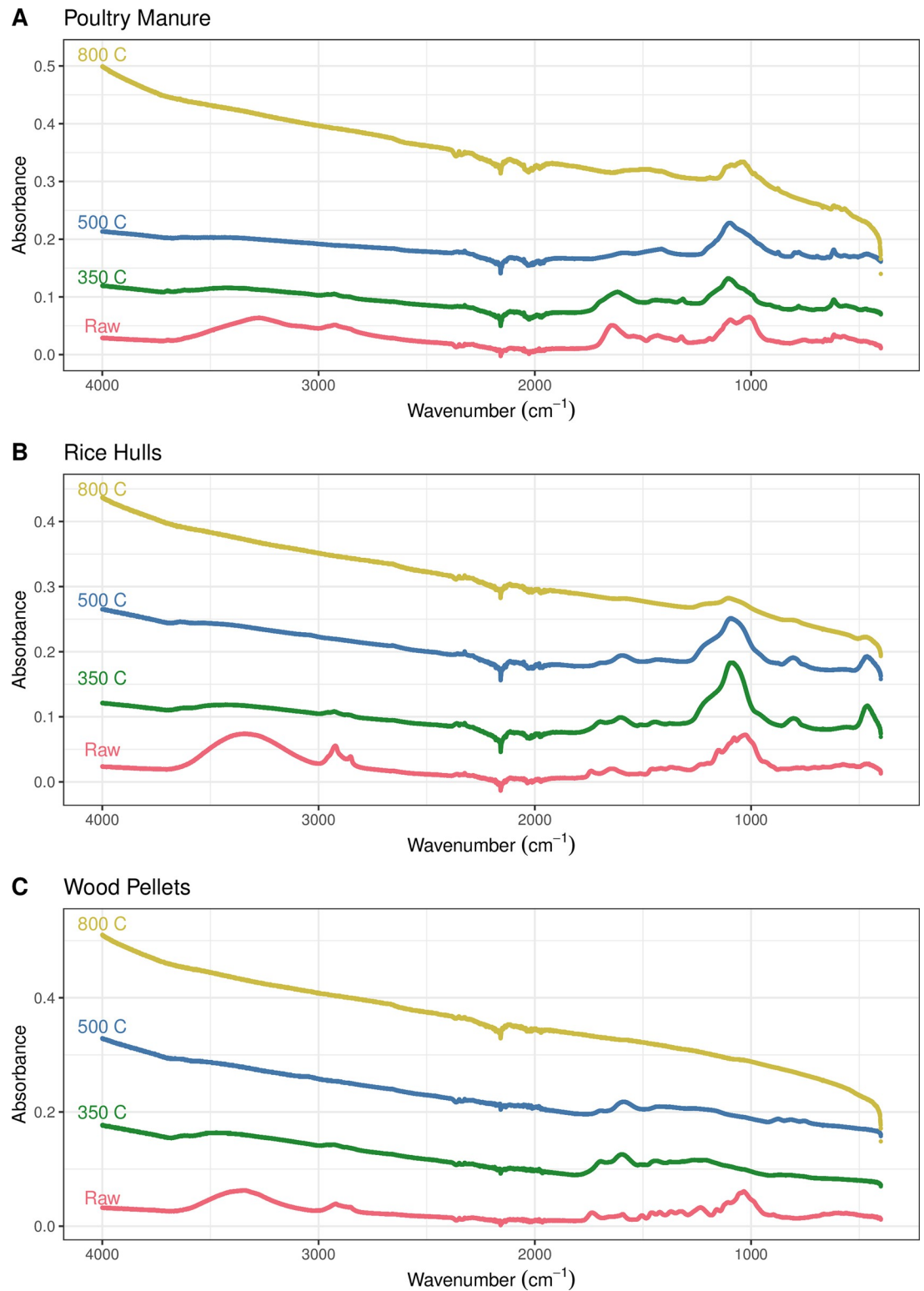
Fig 1. ATR-FTIR spectra for the various samples analyzed in this study, with the data grouped by feedstock (A) poultry manure, (B) rice hulls, and (C) wood pellets with the various pyrolysis treatments displayed in different colors.

https://doi.org/10.1371/journal.pone.0291398.g001

Table 3. Sorption coefficients (Linear, Langmuir, Freundlich, Dubinin–Radushkevich, and Temkin analyses) for MCPA sorption to studied biochars.

	A. Linear Isotherm					
Biochar	Linear Sorption Model (Henry Isotherm Analysis)					
	K_D (mL g^{-1})	SE (mL g^{-1})	AIC	RMSE	R^2	P
PM$_{Raw}$	3.04	0.14	131.17	7.83	0.967	<0.001
PM350	2.82	0.15	133.45	8.34	0.957	<0.001
PM500	7.74	0.41	160.94	17.90	0.954	<0.001
PM800						
RH$_{Raw}$	3.73	0.14	130.72	7.7	0.976	<0.001
RH350	3.01	0.15	133.30	8.3	0.962	<0.001
RH500	5.99	0.32	155.44	15.4	0.952	<0.001
RH800	15.66	1.43	193.29	43.97	0.875	<0.001
WP$_{Raw}$	10.56	0.83	180.7	31.02	0.905	<0.001
WP350	2.96	0.12	125.89	6.75	0.973	<0.001
WP500	2.45	0.21	147.14	12.20	0.890	<0.001
WP800	5.13	0.50	173.01	25.04	0.859	<0.001

Notes: SE–standard error, RMSE—root mean square error, MAE—mean absolute error, AIC—Akaike Information Criterion, BIC—Bayesian Information Criterion, P is the P-value and the corresponding Pearson's correlation (R^2) of the isotherm model fits. Blank values indicate that no model fit was possible of the sorption data.

	B. Langmuir Isotherm						
Biochar	Langmuir Sorption Model (using Langmuiranalysis function)						
	Q_m (µg g^{-1})	K_L (µg g^{-1})	AIC	BIC	MAE	RMSE	R^2
PM$_{Raw}$	423.90	0.01	36.77	36.15	2.21	3.14	1.00
PM350	228.70	0.03	40.00	39.37	3.05	4.11	0.99
PM500	504.18	0.03	50.28	49.66	8.28	9.69	0.99
PM800							
RH$_{Raw}$	3343.00	0.00	40.54	39.92	3.35	4.30	0.99
RH350	246.40	0.02	34.65	34.03	2.01	2.64	1.00
RH500	321.64	0.05	48.14	47.51	6.96	8.11	0.99
RH800	417.19	0.23	57.18	56.56	14.97	17.22	0.99
WP$_{Raw}$	9501.00	0.00	53.70	53.07	9.41	12.88	0.99
WP350	309.20	0.02	43.86	43.23	4.67	5.67	0.98
WP500	156.12	0.05	54.24	53.61	11.35	13.48	0.89
WP800	193.54	0.28	56.81	56.19	12.85	16.70	0.94

Notes: SE–standard error, RMSE—relative mean square error, MAE—mean absolute error (µg g^{-1}), AIC—Akaike Information Criterion, BIC—Bayesian Information Criterion, and the corresponding Pearson's correlation (R^2) of the isotherm model fits. Blank values indicate that no model fit was possible of the sorption data.

	C. Freundlich Isotherm							
Biochar	Freundlich Sorption Model (using Freundlichanalysis function)							
	K_F (mL µg^{-1})	n	$\frac{1}{n}$	AIC	BIC	MAE	RMSE	R^2
PM$_{Raw}$	6.17	1.23	0.81	32.71	32.08	1.80	2.24	1.00
PM350	9.31	1.46	0.68	35.29	34.67	2.32	2.78	0.99
PM500	24.20	1.48	0.68	40.82	40.20	3.41	4.41	1.00

(Continued)

PM800								
RH$_{Raw}$	4.80	1.07	0.94	39.58	38.95	3.09	3.97	0.99
RH350	9.48	1.44	0.70	30.67	30.05	1.53	1.89	1.00
RH500	26.42	1.70	0.59	31.76	31.13	1.95	2.07	1.00
RH800	93.50	2.26	0.44	44.91	44.28	5.58	6.19	1.00
WP$_{Raw}$	6.61	0.86	1.16	50.19	49.57	6.72	9.62	0.99
WP350	8.24	1.37	0.73	39.06	38.43	2.87	3.80	0.99
WP500	14.50	1.87	0.54	50.93	50.31	7.66	10.23	0.91
WP800	49.37	2.60	0.39	49.83	49.20	7.72	9.33	0.98

Notes: SE–standard error, RMSE—root mean square error, MAE—mean absolute error (µg g^{-1}), AIC—Akaike Information Criterion, BIC—Bayesian Information Criterion, P–P-value, and the corresponding Pearson's correlation (R^2) of the isotherm model fits. Blank values indicate that no model fit was possible of the sorption data.

D. Dubinin-Radushkevich Isotherm								
Biochar		**Dubinin–Radushkevich Sorption Model** **(using dubininradushkevichvanalysis function)**						
	Q$_{DR}$ **(µg g^{-1})**	**K$_{DR}$** **(mol^2 J^{-2})**	**E** **(J mol^{-1})**	**AIC**	**BIC**	**MAE**	**RMSE**	**R^2**
PM$_{Raw}$	110.30	1.23E-05	201.6	55.29	54.67	11.71	14.71	0.90
PM350	101.20	7.51E-06	258.0	54.37	53.75	10.19	13.63	0.90
PM500	211.80	4.45E-06	335.2	64.24	63.61	24.89	31.01	0.89
PM800								
RH$_{Raw}$	191.30	6.50E-05	87.7	55.96	55.33	9.27	15.55	0.95
RH350	108.30	8.12E-06	248.1	53.89	53.26	10.09	13.09	0.92
RH500	179.90	3.82E-06	361.8	61.67	61.05	19.70	25.04	0.90
RH800								
WP$_{Raw}$	421.70	4.12E-05	110.2	61.93	61.30	14.50	25.58	0.97
WP350	103.90	8.43E-06	243.5	56.40	55.78	12.54	16.14	0.87
WP500	82.86	2.16E-06	481.1	58.30	57.67	15.25	18.90	0.76
WP800	156.60	5.09E-07	991.1	61.79	61.17	21.62	25.29	0.87

Notes: SE–standard error, RMSE—relative mean square error, MAE—mean absolute error (µg g^{-1}), AIC—Akaike Information Criterion, BIC—Bayesian Information Criterion, P–P-value, and the corresponding Pearson's correlation (R^2) of the isotherm model fits. Blank values indicate that no model fit was possible of the sorption data.

E. Temkin Isotherm							
Biochar		**Temkin Isotherm Analysis** **(using temkinanalysis function)**					
	A$_t$ **(L mg^{-1})**	**B$_t$** **(J mol^{-1})**	**AIC**	**BIC**	**MAE**	**RMSE**	**R^2**
PM$_{Raw}$	3.58	146.01	61.79	60.80	21.83	24.53	0.69
PM350	4.34	152.13	61.79	58.87	18.67	20.89	0.74
PM500	10.91	84.63	61.79	68.42	41.09	46.28	0.71
PM800							
RH$_{Raw}$	3.75	131.88	61.79	63.30	27.04	30.22	0.64
RH350	4.41	145.23	61.79	59.61	19.35	22.22	0.74
RH500	11.84	98.21	61.79	65.35	31.60	35.83	0.76
RH800							
WP$_{Raw}$	4.59	67.48	61.79	72.83	58.61	66.84	0.58
WP350	4.56	151.12	61.79	59.60	19.90	22.19	0.72
WP500	14.75	200.07	61.79	58.10	17.33	19.58	0.73
WP800	66.30	126.01	61.79	62.62	25.78	28.56	0.83

(Continued)

graphite) [78]. The elevated O:C ratios of lower temperature biochars suggest the presence of hydroxyl, carbonyl and carboxylate groups, which could contribute to greater CEC values [79] as CEC values are correlated with the O:C ratios [20]. The O:C ratio decreased drastically over temperature increments also observed in the FTIR data (Fig 1) through the loss of bands for oxygen surface functional groups [20,28]. There was a correlation between O:C and VM content (R = 0.907; P<0.01) and a negative correlation between O:C and fixed carbon (R = -0.811, P<0.05), which also support these conclusions. The PM and RH biochars did possess a peak near 1,100 cm^{-1}, which was present in all the samples to varying degrees, associated with both the P-O bond in phosphate [80] and/or the Si-O bond [81]. This peak has been observed in other PM [82] and RH [83] biochar characterization studies. Additionally, SEM micrographs are presented in the Supplemental Information (S1-S3 Figs in S1 Text).

These results confirm the findings of previous studies which described the dependence of biochar properties on pyrolysis temperature and feedstock [e.g., 84]. These variations in response from different feedstocks, after been subjected to various temperatures, could lead to different outcomes with pesticide sorption. While, on one hand, high pyrolysis temperature could provide more pesticide sorption due to enhanced surface area; on the other hand, reduced functional groups on the biochar surface due to high pyrolysis temperatures could lower pesticide sorption. This was observed in this study by the decreases observed in the estimates from the Langmuir isotherm for the maximum sorbed quantity (Q_m) for MCPA, which had decreases for the biochars for WP and RH feedstocks, regardless of the pyrolysis temperature. The study of these factors on pesticide sorption is therefore necessary to determine a biochar with desirable characteristics for pesticide removal [28].

Sorption results

The raw data are shown in Fig 2, while the estimated parameters for the five sorption models are summarized in Table 3. Examining the resulting linear sorption coefficients (K_D), both feedstock and temperature had a statistically significant effect on the resulting sorption of MCPA (S3 Table in S1 Text; Supplemental Information). K_D for MCPA increased tremendously with increasing pyrolysis temperature from 350 to 800°C. However, only the 800°C was statistically significant (P<0.05; S4 Table in S1 Text).

The resulting individual isotherm model analyses are presented in the Supplemental Information (S4-S16 Figs in S1 Text). Based on the assessment of the AIC criterion [85,86], along with the BIC, MAE, RMSE, and R^2 (Table 3), the Freundlich isotherm model was the best fit describing the nature of MCPA sorption to the various biochars and feedstocks. This would infer that the sorption sites are dissimilatory in their sorption energy [87]. In general, lower pyrolysis temperature typically reduced the estimated sorption capacity (lower K_D and Q_m values), although not statistically significant across all the feedstocks. Except for the PM feedstock, the value of $\frac{1}{n}$ typically decreased with increasing pyrolysis temperatures, indicating a more non-linear behavior of the resulting isotherm and greater heterogeneity of sorption sites (Fig 2). However, direct comparison of the Freundlich coefficients is hampered by differing values of n across the different sorbents [88].

The greater increase in the sorption coefficients of the PM and RH 800°C biochars could be related to the interaction with mineral phases (chemosorption) versus the aromatic carbon
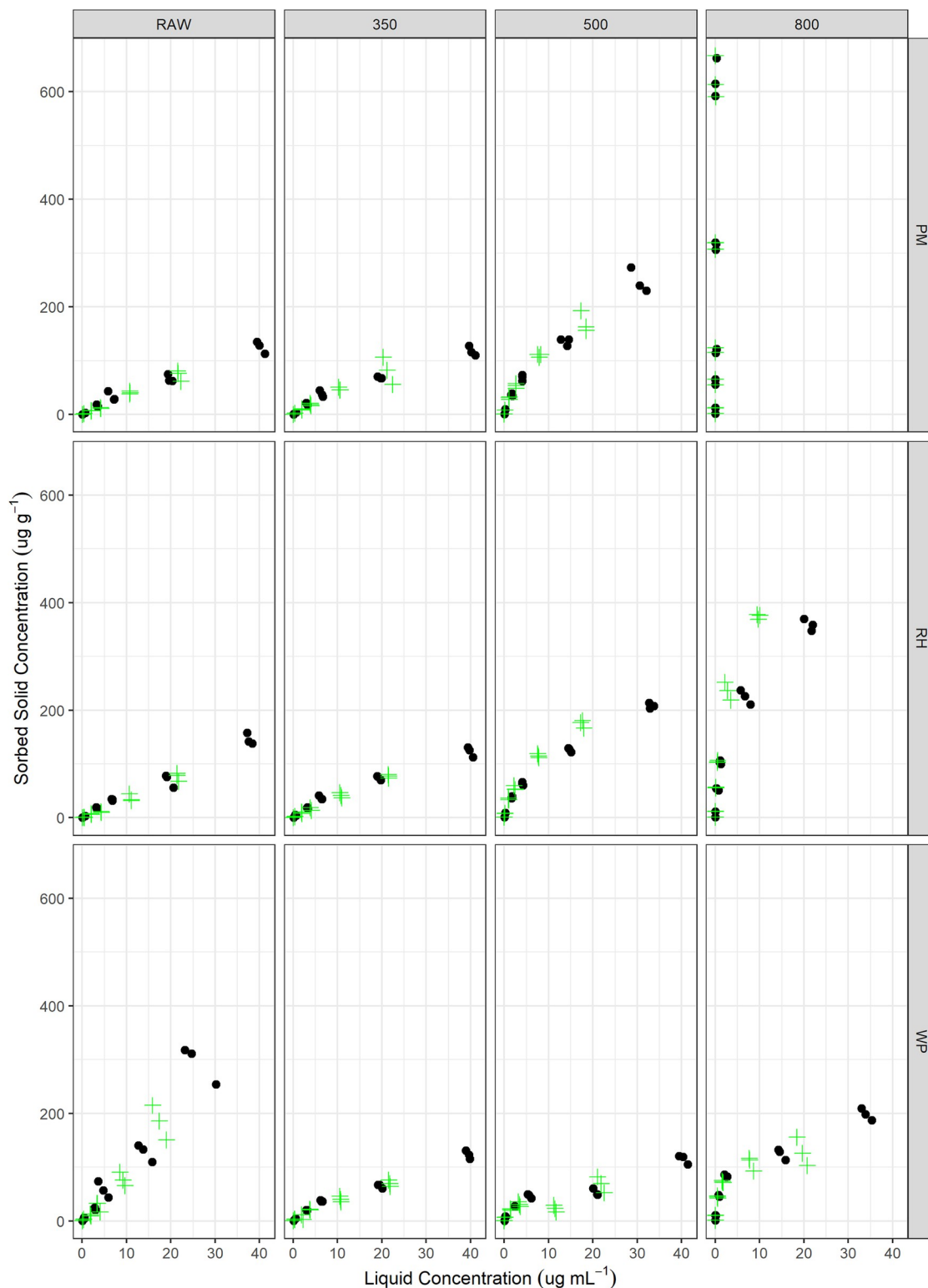
Fig 2. Data for individual sorption and desorption experiments for the three feedstock materials [poultry manure (PM), rice hulls (RH), and wood pellets (WP)] as well as the various pyrolysis temperatures (Raw, 350, 500, and 800°C). The sorption data points are shown with a black dot and the desorption data points are illustrated with the green plus signs.

https://doi.org/10.1371/journal.pone.0291398.g002

orbitals, due to the lack of similar sorption increases with the WP800 biochar (Table 3). Additionally, there is no statistically significant correlation between sorption coefficients and the surface area of the biochar. This would be in agreement with the importance of clay mineral sorption that has been observed in soil matrices [89] and lack of direct correlation of MCPA sorption and soil organic matter (carbon) content [52]. However, no statistically significant correlation was observed between any of the sorption coefficients and the ash content of the various biochars (S3 Table in S1 Text). MCPA has a pK_a of 3.1 (Table 1) and therefore at the pH of the biochar solutions used here (Table 2; pH>6) MCPA would be in the anionic form, which could provide a mechanism for cation interactions [90]. It is also interesting to note that the maximum Langmuir's sorption capacity (Q_m) for MCPA is the highest for the raw feedstocks for the RH and WP, and within the same order of magnitude for the PM treatments (Table 3B). Similarly, the K_D estimated from the linear relationship between Q_s and Q_e (Table 3A) also suggests minimal increases as a function of pyrolysis temperature, except for the PM800 biochar (Table 3A). There was a high sorption capacity observed for the raw WP feedstock (9,501 ug g^{-1}; Table 3B), although the exact mechanisms resulting in this elevated sorption capacity were not elucidated. Overall, the PM800 biochar possessed the highest sorption capacity and removed nearly 100% of the MCPA at all concentrations evaluated here (Fig 2). There was an increasing trend in the estimated free sorption energy from the Dubinin–Radushkevich model (Table 3D) with pyrolysis temperatures. However, we cannot confirm this across all feedstocks due to the lack of fit of the Dubinin–Radushkevich isotherm for PM800 and RH800. This increasing trend in energy would suggest a stronger attraction of MCPA to higher pyrolysis temperatures, but still these values are below those typical for chemosorption (>20 kJ mol^{-1}) [91].

There was a negative correlation with O and VM content and a corresponding positive correlation with H content and H:C ratios with the Langmuir sorption coefficient as well as the Freundlich coefficients, which negates the importance of oxygen surface groups in the sorption mechanisms and highlights potential competitive sorption with VM material already sorbed to the biochars (S17 Fig in S1 Text). The values for the K_D for the feedstocks and biochars (2.8 to 921 L kg^{-1}; Table 3) are greater than those typically observed for MCPA sorption to soils (0.3 to 1.5 L kg^{-1}) [52–55].

Rice residues-based biochars have already been reported to increase sorption capacity for pesticides [26,92–94]. Ren et al. [95] also found better sorption capacity of rice biochar for carbaryl with increasing pyrolysis temperature, with increased sorption obtained at 700˚C. Manna and Singh [94] also reported more pyrazosulfuron-ethyl sorption on higher pyrolysis temperatures. In comparison to 5.3–8.6% pesticide sorption with unamended soil, they recorded 7.5–50.4% and 55.9–91.8% sorption, when amended with biochars pyrolyzed at 400˚C and 600˚C, respectively. Wang et al. [96] had also found higher sorption capability for terbuthylazine by pine wood biochar pyrolyzed at 700˚C, compared with biochar produced at 350˚C, which they linked to higher porosity and surface area for the higher temperature biochar. A wheat straw biochar at 300˚C was observed to have a K_f for MCPA of 43.7 mg^{1-n}kg^{-1}L^n [11] and a switchgrass 425˚C biochar was observed to have a K_f for MCPA of 2.3 mg^{1-n}kg^{-1}L^n [97], which are comparable to those observed in our study (Table 3).

Desorption results

The desorption Freundlich coefficients are shown in Table 4. There was a strong correlation between the sorption coefficients of the sorption models evaluated (K_D, K_L, K_{DR}, A, and K_f) and the desorption K_f (Table 4). Results showed that sorbed MCPA on studied biochars was variably desorbed back to solution depending on the feedstock as well as the concentration

Table 4. Freundlich model coefficients for MCPA desorption from studied biochars and feedstocks.

Biochar	Freundlich Desorption Model (Freundlich Analysis)							
	K_F (mL µg^{-1})	$\frac{1}{n}$	AIC	BIC	MAE	RMSE	R^2	H
PM$_{Raw}$	3.84	0.96	30.82	30.20	1.33	1.91	0.99	1.18
PM350	6.04	0.85	25.48	24.86	1.02	1.23	1.00	1.25
PM500	30.48	0.60	33.93	33.31	2.17	2.48	1.00	0.88
PM800								
RH$_{Raw}$	2.48	1.12	22.67	22.05	0.68	0.97	1.00	1.19
RH350	5.00	0.89	-3.38	-4.01	0.09	0.11	1.00	1.28
RH500	34.77	0.57	34.92	34.30	2.27	2.69	1.00	0.96
RH800	143.20	0.43	50.77	50.14	8.26	10.09	1.00	0.97
WP$_{Raw}$	4.70	1.28	30.36	29.73	1.45	1.84	1.00	1.10
WP350	6.72	0.76	27.21	26.59	0.95	1.42	1.00	1.04
WP500	13.63	0.47	50.43	49.80	7.32	9.81	0.80	0.87
WP800	56.20	0.29	45.36	44.73	5.21	6.43	0.98	0.75

Notes: SE–standard error, RMSE—root mean square error, MAE—mean absolute error(µg g^{-1}), AIC—Akaike Information Criterion, BIC—Bayesian Information Criterion, P–P-value, and the corresponding Pearson's correlation (R^2) of the isotherm model fits. Blank values indicate that no model fit was possible of the sorption data.

level of the herbicide (S5 Table in S1 Text). Among all the twelve testing adsorbers, raw feedstocks possessed weakest sorption of MCPA because a large proportion of initially sorbed herbicide on material surface desorbed back during first desorption cycle (S5 Table in S1 Text), as well as the raw feedstocks possessing the lowest free energy of sorption (E; Table 3D). The reversible sorption from raw feedstock surfaces and from biochars pyrolyzed at low temperatures might be related to the presence of micropores, serving as entrapping sites for pesticide molecules [98,99]. However, MCPA desorption became more irreversible with increases in pyrolysis temperature, as supported by the decreasing values of H (Table 4) and increasing values of E (Table 3). All three feedstocks subjected to the higher temperature of 800°C desorbed back only minute amounts, especially the poultry manure and rice hull based biochars, which produced negative desorption percentages (S5 Table in S1 Text). This demonstrates not only absence of any reversible MCPA sorption, but continued sorption was evident for PM800 and RH800 despite the reduced solution concentrations. All values of H were close to the value of 1, except for the 800°C biochars, which possessed lower H values (Table 4), which suggests some degree of irreversibility in the sorption-desorption of MCPA on the highest temperature biochars. This lack of desorption would be consistent with more chemical-like interactions (i.e., chemosorption) versus physical and/or electrostatic mechanisms. Although this cannot be confirmed due to the lack of isotherm fits (Temkin and Dubinin–Radushkevich) for the PM800 and RH800 samples. Higher desorption of MCPA from raw feedstocks and those of biochar pyrolyzed at low temperatures, particularly rice hulls and wood pellets, could be ascribed to lower energy of sorption resulting from physical and/or electrostatic interactions, reduced surface areas found in these materials [100], or differences in the pH values of the solutions (Table 2).

Conclusion

MCPA sorption differs among feedstocks and biochars behave differently for MCPA sorption depending on the pyrolysis temperature. In general, higher pyrolysis temperatures did increase

the sorption capacity. However, all three raw feedstocks used in this study did have good potential of MCPA sorption (K_D ranging from 3 to 11 mL g^{-1}; Table 3). Raw wood pellets possessed the highest K_D and Q_m of all materials tested here, which also possessed the largest proportion of reversible sorption. This fact would suggest that for MCPA sorption in the field setting, raw WP feedstock would act superior as compared to the biochars created here due to the largest sorption capacity and the reversible nature of the sorption (H = 1.10). This would also reduce overall costs, although the durability of these amendments would be limited due to microbial mineralization. Poultry manure biochar could be regarded as one with superior MCPA sorption properties when subjected to higher pyrolysis temperatures (800˚C). This treatment removed nearly 100% of all the MCPA from solution for the concentrations evaluated and was irreversible sorbed. However, due to the lack of this behavior in the WP800 the removal is hypothesized to be due to the mineral phases (cation bridging) and not the carbon-backbone of the biochar (π-π orbital interactions). This type of biochar (PM800) could be useful when sudden losses of herbicides need to be addressed (e.g., point source leaks, spills) and would increase the economic feasibility of using higher pyrolysis temperatures for this type of remediation versus whole field applications. Pyrolysis temperature should be reduced below 500˚C when biochars are needed to sorb MCPA to reduce field runoff losses associated with heavy irrigation or rainfall. Desorption of herbicides with time will aid in maintaining efficacy for weed control such as those observed in the raw feedstocks or the PM350 or RH350 biochars.

Supporting information

S1 Text. A Microsoft word document containing the supplemental figures and tables as summarized below. S1-S3 Figs Scanning electron micrographs of all the various biochar and feedstock samples used in thus experiment. **S4 Fig** Linear fit of all sorption data. **S5-S7 Figs** Non-linear curve fits the Langmuir sorption models for the 3 different feedstocks. **S8-S10 Figs** Non-linear curve fits the Freundlich sorption models for the 3 different feedstocks. **S11-S13 Figs** Non-linear curve fits the Temkin sorption models for the 3 different feedstocks. **S14-S16 Figs** Non-linear curve fits of the Dubinin–Radushkevich sorption models for the 3 different feedstocks. **S17 Fig**–Correlation matrix for the measured variables. **S1 Table.** Details of liquid additions for each concentration level evaluated. **S2 Table:** Description of sorption model equations and linearized forms used within the PUPAIM package. **S3 Table.** Analysis of variance for the dependence of the feedstock and pyrolysis temperature on the resulted observed values of K_D for the entire experiment. **S4 Table.** Percentage of MCPA desorption from studied biochars. **S5 Table:** ANOVA analysis for sorption coefficient (K_D) and the influence of feedstock and pyrolysis temperature.
(DOCX)

S2 Text. An example R script for generating Langmuir sorption figures in the manuscript from the raw data files in R. Props. xlsx–An EXCEL file with the raw data on the biochar characterization along with the fitted sorption curve coefficients. Used for determining the relationships between biochar properties and sorption coefficients. **MCPA.xlsx**—An Excel datafile with all the collected raw sorption and desorption data. **FTIR.CSV**–A CSV file with the data from the ATR_FTIR analysis.
(TXT)

S1 File.
(CSV)

S2 File.
(XLSX)

S3 File.
(XLSX)

Author Contributions

Conceptualization: Abdullah Niaz, Kurt A. Spokas, Bea Gámiz, David Mulla, Khaliq R. Arshad, Sarfraz Hussain.

Data curation: Abdullah Niaz, Kurt A. Spokas, Bea Gámiz, David Mulla.

Formal analysis: Abdullah Niaz, Kurt A. Spokas, Bea Gámiz, David Mulla, Khaliq R. Arshad.

Funding acquisition: Kurt A. Spokas, Sarfraz Hussain.

Investigation: Abdullah Niaz, Kurt A. Spokas, Bea Gámiz, David Mulla, Khaliq R. Arshad, Sarfraz Hussain.

Methodology: Abdullah Niaz, Kurt A. Spokas, Bea Gámiz, David Mulla, Khaliq R. Arshad, Sarfraz Hussain.

Project administration: Abdullah Niaz, Kurt A. Spokas, David Mulla, Sarfraz Hussain.

Resources: Abdullah Niaz, Kurt A. Spokas, David Mulla, Khaliq R. Arshad.

Software: Kurt A. Spokas.

Supervision: Kurt A. Spokas, David Mulla, Khaliq R. Arshad, Sarfraz Hussain.

Validation: Kurt A. Spokas.

Visualization: Abdullah Niaz, Kurt A. Spokas, Bea Gámiz, David Mulla.

Writing – original draft: Abdullah Niaz, Kurt A. Spokas, Bea Gámiz, David Mulla.

Writing – review & editing: Abdullah Niaz, Kurt A. Spokas, Bea Gámiz, David Mulla, Khaliq R. Arshad, Sarfraz Hussain.

References

1. Rani L, Thapa K, Kanojia N, Sharma N, Singh S, Grewal AS, et al. An extensive review on the consequences of chemical pesticides on human health and environment. Journal of Cleaner Production. 2021; 283:124657.

2. Yu H, Zou W, Chen J, Chen H, Yu Z, Huang J, et al. Biochar amendment improves crop production in problem soils: A review. Journal of Environmental Management. 2019; 232:8–21. https://doi.org/10.1016/j.jenvman.2018.10.117 PMID: 30466010

3. Loos R, Locoro G, Comero S, Contini S, Schwesig D, Werres F, et al. Pan-European survey on the occurrence of selected polar organic persistent pollutants in ground water. Water Res. 2010; 44 (14):4115–26. https://doi.org/10.1016/j.watres.2010.05.032 PMID: 20554303

4. Gilliom R, Barbash J, Crawford C, Hamilton P, Martin J, Nakagaki N, et al. The Quality of Our Nation's Waters—Pesticides in the Nation's Streams and Ground Water 1992–2001: US Geological Survey Circular 1291. Reston, Virginia, USA: US Geological Survey; 2006. p. 172.

5. Piwowarczyk AA, Holden NM. Phenoxyalkanoic acid herbicide sorption and the effect of co-application in a Haplic Cambisol with contrasting management. Chemosphere. 2013; 90(2):535–41. https://doi.org/10.1016/j.chemosphere.2012.08.023 PMID: 22959720

6. Roberts TR, Hutson DH, Lee PW, Nicholls PH, Plimmer JR, Roberts MC, et al. Metabolic pathways of agrochemicals: Part 1: Hebicides and plant growth regulators: Royal Society of Chemistry; 2007. 870 p.

7. Paszko T, Muszyński P, Materska M, Bojanowska M, Kostecka M, Jackowska I. Adsorption and degradation of phenoxyalkanoic acid herbicides in soils: A review. Environmental Toxicology and Chemistry. 2016; 35(2):271–86. https://doi.org/10.1002/etc.3212 PMID: 26292078

8. Bojanowska-Czajka A, Drzewicz P, Zimek Z, Nichipor H, Nałęcz-Jawecki G, Sawicki J, et al. Radiolytic degradation of pesticide 4-chloro-2-methylphenoxyacetic acid (MCPA)—Experimental data and kinetic modelling. Radiat Phys Chem. 2007; 76(11–12):1806–14.

9. Kim S, Chen J, Cheng T, Gindulyte A, He J, He S, et al. PubChem in 2021: new data content and improved web interfaces. Nucleic Acids Res. 2021; 49(D1):D1388–D95. https://doi.org/10.1093/nar/gkaa971 PMID: 33151290

10. PPDB. Pesticide Properties Database Agriculture and Environment Research Unit (AERU) University of Hertfordshire; 2022 [cited 11/30/2022]. Available from: https://sitem.herts.ac.uk/aeru/ppdb/en/index.htm.

11. Hiller E, Khun M, Zemanová L, Jurkovic L, Bartal M. Laboratory study of retention and release of weak acid herbicide MCPA by soils and sediments and leaching potential of MCPA. Plant Soil and Environment. 2006; 52(12):550.

12. Atcheson K, Mellander P-E, Cassidy R, Cook S, Floyd S, McRoberts C, et al. Quantifying MCPA load pathways at catchment scale using high temporal resolution data. Water Res. 2022; 220:118654. https://doi.org/10.1016/j.watres.2022.118654 PMID: 35635916

13. Comoretto L, Arfib B, Chiron S. Pesticides in the Rhône river delta (France): Basic data for a field-based exposure assessment. Science of The Total Environment. 2007; 380(1–3):124–32.

14. García MG, Sánchez JIL, Bravo KAS, Cabal MDC, Pérez-Santín E. Review: Presence, distribution and current pesticides used in Spanish agricultural practices. Science of The Total Environment. 2022; 845:157291. https://doi.org/10.1016/j.scitotenv.2022.157291 PMID: 35835192

15. Schreiner VC, Szöcs E, Bhowmik AK, Vijver MG, Schäfer RB. Pesticide mixtures in streams of several European countries and the USA. Science of The Total Environment. 2016; 573:680–9. https://doi.org/10.1016/j.scitotenv.2016.08.163 PMID: 27589819

16. Ren X, Sun H, Wang F, Zhang P, Zhu H. Effect of aging in field soil on biochar's properties and its sorption capacity. Environmental Pollution. 2018; 242:1880–6. https://doi.org/10.1016/j.envpol.2018.07.078 PMID: 30061080

17. Ali N, Khan S, Yao H, Wang J. Biochars reduced the bioaccessibility and (bio) uptake of organochlorine pesticides and changed the microbial community dynamics in agricultural soils. Chemosphere. 2019; 224:805–15. https://doi.org/10.1016/j.chemosphere.2019.02.163 PMID: 30851532

18. Zhu X, Li J, Xie B, Feng D, Li Y. Accelerating effects of biochar for pyrite-catalyzed Fenton-like oxidation of herbicide 2, 4-D. Chem Eng J. 2020; 391:123605.

19. Regkouzas P, Diamadopoulos E. Adsorption of selected organic micro-pollutants on sewage sludge biochar. Chemosphere. 2019; 224:840–51. https://doi.org/10.1016/j.chemosphere.2019.02.165 PMID: 30852464

20. Mandal A, Singh N, Purakayastha T. Characterization of pesticide sorption behaviour of slow pyrolysis biochars as low cost adsorbent for atrazine and imidacloprid removal. Science of the Total Environment. 2017; 577:376–85. https://doi.org/10.1016/j.scitotenv.2016.10.204 PMID: 27817922

21. Biederman LA, Harpole WS. Biochar and its effects on plant productivity and nutrient cycling: a meta-analysis. GCB bioenergy. 2013; 5(2):202–14.

22. Jeffery S, Verheijen FG, van der Velde M, Bastos AC. A quantitative review of the effects of biochar application to soils on crop productivity using meta-analysis. Agriculture, Ecosystems and Environment. 2011; 144(1):175–87.

23. Lehmann J, Gaunt J, Rondon M. Bio-char sequestration in terrestrial ecosystems–a review. Mitigation and Adaptation Strategies for Global Change. 2006; 11(2):403–27.

24. Kookana RS. The role of biochar in modifying the environmental fate, bioavailability, and efficacy of pesticides in soils: a review. Soil Research. 2010; 48(7):627–37.

25. Waqas M, Asam Z, Rehan M, Anwar M, Khattak RA, Ismail I, et al. Development of biomass-derived biochar for agronomic and environmental remediation applications. Biomass Conversion and Biorefinery. 2021; 11(2):339–61.

26. Wu C, Liu X, Wu X, Dong F, Xu J, Zheng Y. Sorption, degradation and bioavailability of oxyfluorfen in biochar-amended soils. Science of the Total Environment. 2019; 658:87–94. https://doi.org/10.1016/j.scitotenv.2018.12.059 PMID: 30572218

27. Kookana RS, Sarmah AK, Van Zwieten L, Krull E, Singh B. Biochar application to soil: agronomic and environmental benefits and unintended consequences. In: Sparks DL, editor. Advances in Agronomy. 112. San Diego, CA USA: Elsevier Academic Press; 2011. p. 103–43.

28. Liu Y, Lonappan L, Brar SK, Yang S. Impact of biochar amendment in agricultural soils on the sorption, desorption, and degradation of pesticides: a review. Science of the Total Environment. 2018; 645:60–70. https://doi.org/10.1016/j.scitotenv.2018.07.099 PMID: 30015119

29. Yu X-Y, Mu C-L, Gu C, Liu C, Liu X-J. Impact of woodchip biochar amendment on the sorption and dissipation of pesticide acetamiprid in agricultural soils. Chemosphere. 2011; 85(8):1284–9. https://doi.org/10.1016/j.chemosphere.2011.07.031 PMID: 21862101

30. Song Y, Wang F, Bian Y, Kengara FO, Jia M, Xie Z, et al. Bioavailability assessment of hexachlorobenzene in soil as affected by wheat straw biochar. Journal of Hazardous Materials. 2012; 217:391–7. https://doi.org/10.1016/j.jhazmat.2012.03.055 PMID: 22483599

31. Ogram A, Jessup RE, Ou L, Rao P. Effects of sorption on biological degradation rates of (2, 4-dichlorophenoxy) acetic acid in soils. Appl Environ Microbiol. 1985; 49(3):582–7. https://doi.org/10.1128/aem.49.3.582-587.1985 PMID: 3994366

32. Duque-Acevedo M, Belmonte-Urena LJ, Cortés-García FJ, Camacho-Ferre F. Agricultural waste: Review of the evolution, approaches and perspectives on alternative uses. Global Ecology and Conservation. 2020; 22:e00902.

33. Pathak H, Bhatia A, Jain N, Aggarwal P. Greenhouse gas emission and mitigation in Indian agriculture–A review. In: Division of Environmental Sciences IARI, editor. ING bulletins on regional assessment of reactive nitrogen, bulletin. New Delhi, India: INDIAN NITROGEN GROUP (ING) and SOCIETY FOR CONSERVATION OF NATURE (SCON); 2010. p. 1–34.

34. Ogura AP, Lima JZ, Marques JP, Sousa LM, Rodrigues VGS, Espíndola ELG. A review of pesticides sorption in biochar from maize, rice, and wheat residues: Current status and challenges for soil application. Journal of Environmental Management. 2021; 300:113753. https://doi.org/10.1016/j.jenvman.2021.113753 PMID: 34537561

35. Xu C, Liu W, Sheng GD. Burned rice straw reduces the availability of clomazone to barnyardgrass. Science of the Total Environment. 2008; 392(2–3):284–9. https://doi.org/10.1016/j.scitotenv.2007.11.033 PMID: 18178240

36. Acosta R, Fierro V, De Yuso AM, Nabarlatz D, Celzard A. Tetracycline adsorption onto activated carbons produced by KOH activation of tyre pyrolysis char. Chemosphere. 2016; 149:168–76. https://doi.org/10.1016/j.chemosphere.2016.01.093 PMID: 26855221

37. Antón-Herrero R, García-Delgado C, Alonso-Izquierdo M, García-Rodríguez G, Cuevas J, Eymar E. Comparative adsorption of tetracyclines on biochars and stevensite: Looking for the most effective adsorbent. Applied Clay Science. 2018; 160:162–72.

38. Rajapaksha AU, Chen SS, Tsang DC, Zhang M, Vithanage M, Mandal S, et al. Engineered/designer biochar for contaminant removal/immobilization from soil and water: potential and implication of biochar modification. Chemosphere. 2016; 148:276–91. https://doi.org/10.1016/j.chemosphere.2016.01.043 PMID: 26820777

39. Tan X-f, Liu Y-g, Gu Y-l, Xu Y, Zeng G-m, Hu X-j, et al. Biochar-based nano-composites for the decontamination of wastewater: A review. Bioresource Technology. 2016; 212:318–33. https://doi.org/10.1016/j.biortech.2016.04.093 PMID: 27131871

40. Yan L, Kong L, Qu Z, Li L, Shen G. Magnetic biochar decorated with ZnS nanocrytals for Pb (II) removal. ACS Sustainable Chemistry and Engineering. 2015; 3(1):125–32.

41. Tang J, Lv H, Gong Y, Huang Y. Preparation and characterization of a novel graphene/biochar composite for aqueous phenanthrene and mercury removal. Bioresource Technology. 2015; 196:355–63. https://doi.org/10.1016/j.biortech.2015.07.047 PMID: 26255599

42. Cantrell KB, Hunt PG, Uchimiya M, Novak JM, Ro KS. Impact of pyrolysis temperature and manure source on physicochemical characteristics of biochar. Bioresource technology. 2012; 107:419–28. https://doi.org/10.1016/j.biortech.2011.11.084 PMID: 22237173

43. Chen T, Zhang Y, Wang H, Lu W, Zhou Z, Zhang Y, et al. Influence of pyrolysis temperature on characteristics and heavy metal adsorptive performance of biochar derived from municipal sewage sludge. Bioresource technology. 2014; 164:47–54. https://doi.org/10.1016/j.biortech.2014.04.048 PMID: 24835918

44. Liu Y, Yao S, Wang Y, Lu H, Brar SK, Yang S. Bio-and hydrochars from rice straw and pig manure: inter-comparison. Bioresource Technology. 2017; 235:332–7. https://doi.org/10.1016/j.biortech.2017.03.103 PMID: 28376384

45. Yavari S, Malakahmad A, Sapari NB. Biochar efficiency in pesticides sorption as a function of production variables—a review. Environmental Science and Pollution Research. 2015; 22(18):13824–41. https://doi.org/10.1007/s11356-015-5114-2 PMID: 26250816

46. Atkinson CJ, Fitzgerald JD, Hipps NA. Potential mechanisms for achieving agricultural benefits from biochar application to temperate soils: a review. Plant and soil. 2010; 337(1):1–18.

47. Keiluweit M, Nico PS, Johnson MG, Kleber M. Dynamic molecular structure of plant biomass-derived black carbon (biochar). Environmental Science & Technology. 2010; 44(4):1247–53. https://doi.org/10.1021/es9031419 PMID: 20099810

48. Loganathan VA, Feng Y, Sheng GD, Clement TP. Crop-residue-derived char influences sorption, desorption and bioavailability of atrazine in soils. Soil Science Society of America Journal. 2009; 73 (3):967–74.

49. Nag SK, Kookana R, Smith L, Krull E, Macdonald LM, Gill G. Poor efficacy of herbicides in biochar-amended soils as affected by their chemistry and mode of action. Chemosphere. 2011; 84(11):1572–7. https://doi.org/10.1016/j.chemosphere.2011.05.052 PMID: 21696801

50. Eibisch N, Schroll R, Fuß R, Mikutta R, Helfrich M, Flessa H. Pyrochars and hydrochars differently alter the sorption of the herbicide isoproturon in an agricultural soil. Chemosphere. 2015; 119:155–62. https://doi.org/10.1016/j.chemosphere.2014.05.059 PMID: 24974225

51. Soni N, Leon RG, Erickson JE, Ferrell JA, Silveira ML. Biochar decreases atrazine and pendimethalin preemergence herbicidal activity. Weed Technol. 2015; 29(3):359–66.

52. Haberhauer G, Pfeiffer L, Gerzabek M, Kirchmann H, Aquino A, Tunega D, et al. Response of sorption processes of MCPA to the amount and origin of organic matter in a long-term field experiment. European Journal of Soil Science. 2001; 52(2):279–86.

53. Jensen PH, Hansen HCB, Rasmussen J, Jacobsen OS. Sorption-controlled degradation kinetics of MCPA in soil. Environmental Science and Technology. 2004; 38(24):6662–8. https://doi.org/10.1021/es0494095 PMID: 15669325

54. Helweg A. Degradation and adsorption of 14C-MCPA in soil—Influence of concentration, temperature and moisture content on degradation. Weed Res. 1987; 27(4):287–96.

55. Thorstensen CW, Lode O, Eklo OM, Christiansen A. Sorption of bentazone, dichlorprop, MCPA, and propiconazole in reference soils from Norway. Journal of Environmental Quality. 2001; 30(6):2046–52. https://doi.org/10.2134/jeq2001.2046 PMID: 11790012

56. Brunauer S, Emmett PH, Teller E. Adsorption of gases in multimolecular layers. J Am Chem Soc. 1938; 60(2):309–19. https://doi.org/10.1021/ja01269a023

57. Barrett EP, Joyner LG, Halenda PP. The determination of pore volume and area distributions in porous substances. I. Computations from nitrogen isotherms. J Am Chem Soc. 1951; 73(1):373–80. https://doi.org/10.1021/ja01145a126

58. Cabrera A, Cox L, Spokas KA, Celis R, Hermosín MC, Cornejo J, et al. Comparative sorption and leaching study of the herbicides fluometuron and 4-chloro-2-methylphenoxyacetic acid (MCPA) in a soil amended with biochars and other sorbents. Journal of agricultural and food chemistry. 2011; 59 (23):12550–60. https://doi.org/10.1021/jf202713q PMID: 22023336

59. Ostan KT, Manlapaz PAC, Mesias JCL, Deocaris CC. PUPAIM: A Collection of Physical and Chemical Adsorption Isotherm Models. R package Version 0.3.1 2022 [cited 2022 12/7/2022]. Available from: https://CRAN.R-project.org/package=PUPAIM.

60. Foo KY, Hameed BH. Insights into the modeling of adsorption isotherm systems. Chem Eng J. 2010; 156(1):2–10. https://doi.org/10.1016/j.cej.2009.09.013.

61. Weber TW, Chakravorti RK. Pore and solid diffusion models for fixed-bed adsorbers. AICHE J. 1974; 20(2):228–38. https://doi.org/10.1002/aic.690200204.

62. Baláž P, Aláčová A, Briančin J. Sensitivity of Freundlich equation constant 1/n for zinc sorption on changes induced in calcite by mechanical activation. Chem Eng J. 2005; 114(1):115–21. https://doi.org/10.1016/j.cej.2005.08.017.

63. Ayawei N, Ebelegi AN, Wankasi D. Modelling and interpretation of adsorption isotherms. Journal of Chemistry. 2017; 2017:3039817. https://doi.org/10.1155/2017/3039817

64. Nguyen C, Do DD. The Dubinin-Radushkevich equation and the underlying microscopic adsorption description. Carbon. 2001; 39:1327–36. https://doi.org/10.1016/S0008-6223(00)00265-7

65. Celis R, Koskinen WC, Hermosín MC, Cornejo J. Sorption and desorption of triadimefon by soils and model soil colloids. Journal of Agricultural and Food Chemistry. 1999; 47(2):776–81. https://doi.org/10.1021/jf980618g PMID: 10563968

66. Team RC. R: A Language and Environment for Statistical Computing. Foundation for Statistical Computing, Available at: https://www.R-project.org/. Vienna, Austria 2019.

67. Kassambara A. ggcorrplot: Visualization of a Correlation Matrix using 'ggplot2'. R package version 0.1.4. 2022 [cited 2022 12/5/2022]. Available from: https://CRAN.R-project.org/package=ggcorrplot.

68. Fd Mendiburu. Agricolae: Statistical Procedures for Agricultural Research, R package version 1.3–5 2021 [cited 2022]. Available from: https://CRAN.R-project.org/package=agricolae.

69. Bagreev A, Bandosz TJ, Locke DC. Pore structure and surface chemistry of adsorbents obtained by pyrolysis of sewage sludge-derived fertilizer. Carbon. 2001; 39(13):1971–9.

70. Guo Y, Du E. The effects of thermal regeneration conditions and inorganic compounds on the characteristics of activated carbon used in power plant. Energy Procedia. 2012; 17:444–9.

71. Heitkötter J, Marschner B. Interactive effects of biochar ageing in soils related to feedstock, pyrolysis temperature, and historic charcoal production. Geoderma. 2015; 245:56–64.

72. Jin J, Li Y, Zhang J, Wu S, Cao Y, Liang P, et al. Influence of pyrolysis temperature on properties and environmental safety of heavy metals in biochars derived from municipal sewage sludge. Journal of Hazardous Materials. 2016; 320:417–26. https://doi.org/10.1016/j.jhazmat.2016.08.050 PMID: 27585274

73. Yuan J-H, Xu R-K, Zhang H. The forms of alkalis in the biochar produced from crop residues at different temperatures. Bioresource Technology. 2011; 102(3):3488–97. https://doi.org/10.1016/j.biortech.2010.11.018 PMID: 21112777

74. Li H, Dong X, da Silva EB, de Oliveira LM, Chen Y, Ma LQ. Mechanisms of metal sorption by biochars: biochar characteristics and modifications. Chemosphere. 2017; 178:466–78. https://doi.org/10.1016/j.chemosphere.2017.03.072 PMID: 28342995

75. Mozzetti Monterumici C, Rosso D, Montoneri E, Ginepro M, Baglieri A, Novotny EH, et al. Processed vs. non-processed biowastes for agriculture: effects of post-harvest tomato plants and biochar on radish growth, chlorophyll content and protein production. International Journal of Molecular Sciences. 2015; 16(4):8826–43. https://doi.org/10.3390/ijms16048826 PMID: 25906472

76. Cely P, Tarquis A, Paz-Ferreiro J, Mendez A, Gasco G. Factors driving the carbon mineralization priming effect in a sandy loam soil amended with different types of biochar. Solid Earth. 2014; 5(1):585–94.

77. Jariwala BN, Ciobanu CV, Agarwal S. Atomic hydrogen interactions with amorphous carbon thin films. Journal of Applied Physics. 2009; 106(7):073305.

78. Ţucureanu V, Matei A, Avram AM. FTIR Spectroscopy for Carbon Family Study. Crit Rev Anal Chem. 2016; 46(6):502–20. https://doi.org/10.1080/10408347.2016.1157013 PMID: 26941009

79. Lee JW, Kidder M, Evans BR, Paik S, Buchanan Iii A, Garten CT, et al. Characterization of biochars produced from cornstovers for soil amendment. Environmental Science and Technology. 2010; 44(20):7970–4. https://doi.org/10.1021/es101337x PMID: 20836548

80. Daasch L, Smith D. Infrared spectra of phosphorus compounds. Analytical Chemistry. 1951; 23(6):853–68. https://doi.org/10.1021/ac60054a008

81. Larkin PJ. Chapter 8—Illustrated IR and Raman Spectra Demonstrating Important Functional Groups. In: Larkin PJ, editor. Infrared and Raman Spectroscopy (Second Edition): Elsevier; 2018. p. 153–210.

82. Liu Y, He Z, Uchimiya M. Comparison of biochar formation from various agricultural by-products using FTIR spectroscopy. Modern Applied Science. 2015; 9:246–53. https://doi.org/10.5539/mas.v9n4p246

83. Xu X, Cao X, Zhao L. Comparison of rice husk- and dairy manure-derived biochars for simultaneously removing heavy metals from aqueous solutions: Role of mineral components in biochars. Chemosphere. 2013; 92(8):955–61. https://doi.org/10.1016/j.chemosphere.2013.03.009 PMID: 23591132

84. Li S, Harris S, Anandhi A, Chen G. Predicting biochar properties and functions based on feedstock and pyrolysis temperature: A review and data syntheses. Journal of Cleaner Production. 2019; 215:890–902.

85. Burnham KP, Anderson DR. Multimodel inference: Understanding AIC and BIC in model selection. Sociological Methods and Research. 2004; 33(2):261–304. https://doi.org/10.1177/0049124104268644

86. Rajahmundry GK, Garlapati C, Kumar PS, Alwi RS, Vo D-VN. Statistical analysis of adsorption isotherm models and its appropriate selection. Chemosphere. 2021; 276:130176. https://doi.org/10.1016/j.chemosphere.2021.130176 PMID: 33714156

87.   Suzuki M. Adsorption Engineering. Churchill SW, editor. New York, NY: Kodansha Tokyo and Elsevier Publishers; 1990. 660 p.

88.   Carmo AM, Hundal LS, Thompson ML. Sorption of hydrophobic organic compounds by soil materials: Application of unit equivalent Freundlich coefficients. Environmental Science & Technology. 2000; 34 (20):4363–9. https://doi.org/10.1021/es000968v

89.   Inacio J, Taviot-Guého C, Forano C, Besse JP. Adsorption of MCPA pesticide by MgAl-layered double hydroxides. Applied Clay Science. 2001; 18(5):255–64. https://doi.org/10.1016/S0169-1317(01) 00029-1.

90.   Iglesias A, López R, Gondar D, Antelo J, Fiol S, Arce F. Adsorption of MCPA on goethite and humic acid-coated goethite. Chemosphere. 2010; 78(11):1403–8. https://doi.org/10.1016/j.chemosphere. 2009.12.063 PMID: 20083293

91.   Saleh TA. Chapter 2—Adsorption technology and surface science. In: Saleh TA, editor. Interface Science and Technology. 34: Elsevier; 2022. p. 39–64.

92.   Aldana GO, Hazlerigg C, Lopez-Capel E, Werner D. Agrochemical leaching reduction in biochar-amended tropical soils of Belize. European Journal of Soil Science. 2021; 72(3):1243–55.

93.   Lü J, Li J, Li Y, Chen B, Bao Z. Use of rice straw biochar simultaneously as the sustained release carrier of herbicides and soil amendment for their reduced leaching. Journal of Agricultural and Food Chemistry. 2012; 60(26):6463–70. https://doi.org/10.1021/jf3009734 PMID: 22686323

94.   Manna S, Singh N. Effect of wheat and rice straw biochars on pyrazosulfuron-ethyl sorption and persistence in a sandy loam soil. Journal of Environmental Science and Health, Part B. 2015; 50(7):463–72.

95.   Ren X, Zhang P, Zhao L, Sun H. Sorption and degradation of carbaryl in soils amended with biochars: influence of biochar type and content. Environmental Science and Pollution Research. 2016; 23 (3):2724–34. https://doi.org/10.1007/s11356-015-5518-z PMID: 26438372

96.   Wang H, Lin K, Hou Z, Richardson B, Gan J. Sorption of the herbicide terbuthylazine in two New Zealand forest soils amended with biosolids and biochars. J Soils Sed. 2010; 10(2):283–9.

97.   Tatarková V, Hiller E, Vaculík M. Impact of wheat straw biochar addition to soil on the sorption, leaching, dissipation of the herbicide (4-chloro-2-methylphenoxy)acetic acid and the growth of sunflower (*Helianthus annuus L.*). Ecotoxicol Environ Saf. 2013; 92:215–21. https://doi.org/10.1016/j.ecoenv. 2013.02.005.

98.   Yu X, Pan L, Ying G, Kookana RS. Enhanced and irreversible sorption of pesticide pyrimethanil by soil amended with biochars. Journal of Environmental Sciences. 2010; 22(4):615–20. https://doi.org/10. 1016/s1001-0742(09)60153-4 PMID: 20617740

99.   Yu X-Y, Ying G-G, Kookana RS. Sorption and desorption behaviors of diuron in soils amended with charcoal. Journal of Agricultural and Food Chemistry. 2006; 54(22):8545–50. https://doi.org/10.1021/ jf061354y PMID: 17061832

100.   Khorram MS, Wang Y, Jin X, Fang H, Yu Y. Reduced mobility of fomesafen through enhanced adsorption in biochar-amended soil. Environ Toxicol Chem. 2015; 34(6):1258–66. https://doi.org/10.1002/ etc.2946 PMID: 25703508